THE JOURNAL OF BIOLOGICAL CHEMISTRY
Vol. 279, No. 29, Issue of July 16, pp. 30279–30286, 2004

Printed in U.S.A.

Visualization of G Protein βγ Dimers Using Bimolecular Fluorescence Complementation Demonstrates Roles for Both β and γ in Subcellular Targeting*[S]

Received for publication, February 9, 2004, and in revised form, May 3, 2004
Published, JBC Papers in Press, May 10, 2004, DOI 10.1074/jbc.M401432200

Thomas R. Hynes‡, Linnan Tang§, Stacy M. Mervine‡, Jonathan L. Sabo‡, Evan A. Yost‡, Peter N. Devreotes§, and Catherine H. Berlot‡¶

From the ‡The Weis Center for Research, Geisinger Clinic, Danville, Pennsylvania 17822-2623 and §The Department of Cell Biology, Johns Hopkins University School of Medicine, Baltimore, Maryland 21205

To investigate the role of subcellular localization in regulating the specificity of G protein βγ signaling, we have applied the strategy of bimolecular fluorescence complementation (BiFC) to visualize βγ dimers *in vivo*. We fused an amino-terminal yellow fluorescent protein fragment to β and a carboxyl-terminal yellow fluorescent protein fragment to γ. When expressed together, these two proteins produced a fluorescent signal in human embryonic kidney 293 cells that was not obtained with either subunit alone. Fluorescence was dependent on βγ assembly in that it was not obtained using β_2 and γ_1, which do not form a functional dimer. In addition to assembly, BiFC βγ complexes were functional as demonstrated by more specific plasma membrane labeling than was obtained with individually tagged fluorescent β and γ subunits and by their abilities to potentiate activation of adenylyl cyclase by α_s in COS-7 cells. To investigate isoform-dependent targeting specificity, the localization patterns of dimers formed by pair-wise combinations of three different β subunits with three different γ subunits were compared. BiFC βγ complexes containing either β_1 or β_2 localized to the plasma membrane, whereas those containing β_5 accumulated in the cytosol or on intracellular membranes. These results indicate that the β subunit can direct trafficking of the γ subunit. Taken together with previous observations, these results show that the G protein α, β, and γ subunits all play roles in targeting each other. This method of specifically visualizing βγ dimers will have many applications in sorting out roles for particular βγ complexes in a wide variety of cell types.

More than a thousand G protein-coupled receptors play roles in a vast range of biological processes. An important but poorly understood issue is how signaling specificity is maintained *in vivo*. Most combinations of the 5 G protein β subunits and 12 γ subunits that have been identified in mammals (1) can form dimers *in vitro* that exhibit similar abilities to modulate the activities of effectors such as adenylyl cyclase (2), phospholipase C (3), and G protein-gated inwardly rectifying K^+ channels (4). However, emerging evidence suggests that the specificity of receptor-G protein signaling is determined by specific αβγ combinations (5). Inactivation of specific G protein subunits *in vivo* using antisense (6–10) and ribozyme (11, 12) strategies has demonstrated a remarkable specificity of interaction between receptors, αβγ combinations, and effectors. For instance, ribozyme-mediated suppression of γ_7 in HEK-293 cells specifically reduces expression of β_1 and disrupts activation of G_s by β-adrenergic, but not prostaglandin E_1 receptors (11, 12). Knockout of γ_7 in the mouse results in behavioral changes and reductions in the level of α_{olf} in the striatum (13).

Reconstitution experiments indicate clear differences in the αβγ combinations that are preferred by particular receptors (14–18). However, these differences generally do not appear to be great enough to account for the large effects seen with *in vivo* knockout models such as the γ_7-deficient mouse (13). In addition, studies of how G protein subunits are organized and localized *in vivo* suggest that cell type-specific expression and subcellular localization also play major roles in signaling specificity (19). In support of this idea, rescue of α_s and α_q mutants with decreased affinities for βγ by co-expressed βγ dimers indicates differences in the abilities of particular βγ dimers to target these α subunits to the plasma membrane (20).

The G protein subunits are peripheral membrane proteins that associate with the plasma membrane as a result of fatty acid modifications and interaction with each other. Targeting of β subunits to the plasma membrane requires association with prenylated γ subunits (21). α subunits attach to the plasma membrane as a result of amino-terminal palmitoylation and/or myristoylation and association with βγ subunits (22). A γ subunit that is mislocalized to the mitochondria can cause α and β to mislocalize (23). Conversely, when α_s is targeted to the mitochondria, $\beta_1\gamma_2$ follows (24). A role for the β subunit in targeting G proteins has not been reported.

Here we apply the strategy of bimolecular fluorescence complementation (BiFC)[1] (25) to visualize specific βγ dimers *in vivo*. BiFC involves the production of a fluorescent signal by two nonfluorescent fragments of YFP when they are brought together by interactions between proteins fused to each fragment. We fused an amino-terminal YFP fragment to β and a carboxyl-terminal YFP fragment to γ. When expressed together, these two proteins produce a fluorescent signal in HEK-293 cells that is not obtained with either subunit alone. This

* This work was supported by National Institutes of Health Grant GM50369. The costs of publication of this article were defrayed in part by the payment of page charges. This article must therefore be hereby marked "*advertisement*" in accordance with 18 U.S.C. Section 1734 solely to indicate this fact.

[S] The on-line version of this article (available at http://www.jbc.org) contains Supplemental Video 1.

¶ To whom correspondence should be addressed: The Weis Center for Research, Geisinger Clinic, 100 North Academy Ave., Danville, PA 17822-2623. Tel.: 570-271-8661; Fax: 570-271-6701; E-mail: chberlot@geisinger.edu.

[1] The abbreviations used are: BiFC, bimolecular fluorescence complementation; GFP, green fluorescent protein; YFP, yellow fluorescent protein; CFP, cyan fluorescent protein; mRFP, monomeric red fluorescent protein; HEK cells, human embryonic kidney cells; ECFP, enhanced CFP; RGS, regulator of G protein signaling.

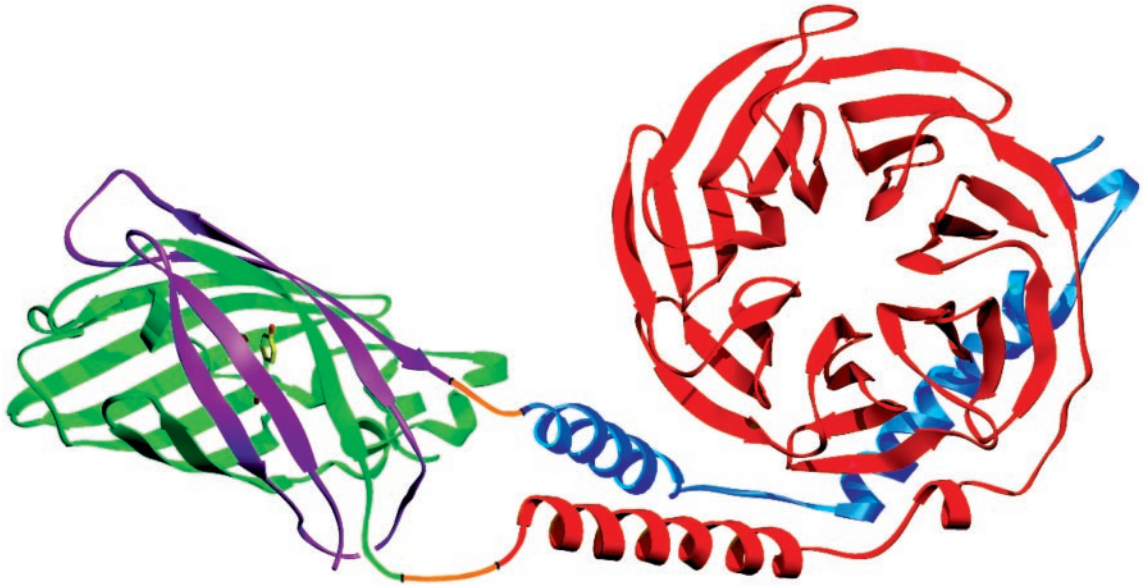

FIG. 1. **Model of YFP-N-β·YFP-C-γ.** YFP-N (*green*) is fused to the G protein β subunit (*red*), and YFP-C (*magenta*) is fused to the G protein γ subunit (*blue*). Linker sequences between the YFP fragments and the G protein subunits are *orange*. The structures of YFP-N and YFP-C are adapted from the structure of GFP (54). The structures of β and γ are from the structure of an α_t/α_{i1} chimera complexed with $\beta_t\gamma_t$ (55).

procedure enables visualization of βγ pairs that form complexes, producing no fluorescence for a βγ combination known to be unable to assemble. BiFC βγ complexes were functional, as demonstrated by more specific plasma membrane labeling than was obtained with individually tagged fluorescent β and γ subunits and by their abilities to modulate adenylyl cyclase activity. Comparisons of the localization patterns of βγ complexes formed by pairwise combinations of three different β subunits with three different γ subunits showed clear differences in localization patterns. This study also showed that the β subunit can direct βγ targeting in that complexes containing either β_1 or β_2 localized to the plasma membrane, whereas those containing β_5 accumulated in the cytosol or on intracellular membranes. This method of specifically visualizing βγ dimers will have many applications in sorting out the roles of particular βγ complexes in a wide variety of cells and tissues.

EXPERIMENTAL PROCEDURES

Production of Fluorescent Fusion Proteins—To produce YFP-(1–158)β_1 in pcDNAI/Amp, YFP-(1–158) was amplified by a PCR from enhanced YFP (Clontech) that introduced a substitution of Met for Gln-69 (26). The PCR introduced a BamHI site at the 5′ end of YFP-(1–158) and a BglII site at the 3′ end. A BglII site was introduced into the polylinker of pcDNAI/Amp 3′ to the BamHI site, and YFP-(1–158) was subcloned into these sites to produce YFP-(1–158)pcDNAI/Amp. A BglII site in the human β_1 cDNA[2] was removed using the QuikChange site-directed mutagenesis kit (Stratagene), and the cDNA was amplified by a PCR that added a linker sequence (Arg-Ser-Ile-Ala-Thr) containing a BamHI site on the 5′ end and a BglII site on the 3′ end. This PCR product was digested with BamHI and BglII and subcloned into the BglII site of YFP-(1–158)pcDNAI/Amp so that YFP-(1–158) was fused to the amino terminus of β_1. To produce YFP-(1–158)β_2 and YFP-(1–158)β_5 in pcDNAI/Amp, the human β_2 cDNA[2] and the human β_5 cDNA were each amplified by PCR, digested with BamHI and BglII, and subcloned into the BglII site of YFP-(1–158)pcDNAI/Amp as described for β_1.

A similar strategy was used to produce YFP-(159–238)γ_7. YFP-(159–238) was amplified from enhanced YFP by a PCR that introduced a BamHI site at the 5′ end of YFP-(159–238) and a BglII site at the 3′ end and subcloned into the BamHI and BglII sites of the modified pcDNAI/Amp vector described above to produce YFP-(159–238)pcDNAI/Amp. The human γ_7 cDNA (27) was amplified by a PCR that added a BamHI site and a linker sequence (Arg-Ser) to the 5′ end and a BglII site to the 3′ end. This PCR product was digested with BamHI and BglII and subcloned into the BglII site of YFP-(159–238)pcDNAI/Amp so that YFP-(159–238) was fused to the amino terminus of γ_7. To produce YFP-(159–238)γ_1 and YFP-(159–238)γ_2, the bovine γ_1 cDNA[2] and the human γ_2 cDNA (27) were each amplified by PCR, digested with BamHI and BglII, and subcloned into the BglII site of YFP-(159–238)pcDNAI/Amp as described for γ_7.

YFP-N-β and YFP-C-γ in the *Dictyostelium* expression vector pCV5 were produced as follows. For YFP-N-β, PCR of YFP-(1–158) introduced a BamHI site followed by a *Dictyostelium* ribosomal binding site at the 5′ end and a BglII site at the 3′ end. The *Dictyostelium* β-coding sequence was amplified with introduction of a BamHI site and a linker sequence (Ile-Ala-Thr) at the 5′ end and a BglII site at 3′ end. The two PCR fragments were sequentially subcloned into the BglII site in pCV5. For YFP-C-γ, a BamHI site and the codons for Met-Ser were introduced before YFP-(159–238), and the YFP stop codon was eliminated and substituted with a BglII site. The *Dictyostelium* γ subunit-coding sequence was flanked by a BamHI site on the 5′ end and a BglII site on the 3′ end. These two fragments were sequentially subcloned into pCV5.

To produce GFP-β_1, the human β_1 cDNA was amplified by PCR and ligated into pWay5, a derivative of pCR3.1 (Invitrogen), in the presence of Srf I, as described (28). This procedure added a linker sequence (Gly-Gly-Gly-Pro-Ser-Gly-Gly-Gly-Gly-Ser) in between the amino-terminal GFP and the carboxyl-terminal β_1 sequences.

To produce CFP-γ_2 and CFP-γ_7, the GFP sequence in pWAY5 was replaced with that of ECFP (Clontech) containing a substitution of His for Asn-164 (29), and the γ_2 and γ_7 sequences were each amplified by PCR and subcloned into this vector in the presence of Srf I. The resulting constructs contained a linker sequence (Gly-Gly-Gly-Pro-Tyr-Pro-Tyr-Asp-Val-Pro-Asp-Tyr-Ala-Ser-Leu-Gly-Gly-Pro-Gly-Ile-Leu-Arg) that includes the hemagglutinin epitope in between the ECFP and γ sequences, similar to that described in Manahan *et al.* (30). All constructs were verified by DNA sequencing.

Transient Expression and Assay for cAMP Accumulation—0.8×10^6 COS-7 cells (obtained from Henry Bourne) in 60-mm dishes were transfected with plasmids as described in the legends to Figs. 3 and 4 using 10 μl of LipofectAMINE 2000 reagent (Invitrogen) according to the manufacturer's instructions. 24 h after transfection, the cells were replated in 24-well plates and labeled with [^{3}H]adenine. After an additional 24 h, intracellular cAMP levels were determined as described previously (31). cAMP accumulation was measured in the presence of 1 mM 3-isobutyl-1-methylxanthine, a phosphodiesterase inhibitor.

Imaging of Fluorescent Fusion Proteins—HEK-293 cells (ATCC, CRL-1573) were plated at a density of 10^5 cells per well on Lab-Tek II 4-well chambered coverslips and transiently transfected with 0.075 μg each of plasmids encoding YFP-N-β and YFP-C-γ constructs and 0.0125 μg each of pECFP-Mem (Clontech), which encodes a fluorescent fusion protein targeted to the plasma membrane by the amino-terminal 20 residues of neuromodulin (32), and mRFP, expressed in pcDNA3 (33) as

[2] J. Robishaw, unpublished information.

a marker for the cytosol, using 0.25 μl of LipofectAMINE 2000 Reagent (Invitrogen). For studies of GFP-β_1, CFP-γ_2, and CFP-γ_7, cells were transfected with 0.075 μg each of fluorescent and/or untagged G protein subunits, as described in the legend to Fig. 4. The cells were imaged 2 days after transfection at 63× using a Zeiss Axiovert 200 fluorescence microscope equipped with computer-controlled filter wheels, shutters, xyz stage (Ludl), and an ORCA-ER camera (Hamamatsu) under the control of IPLab software (Scanalytics). A single triple pass dichroic mirror (86006bs, Chroma) was used to ensure image registration. Excitation and emission filters for CFP (430/25, 465/30), YFP (495/20, 535/25), and mRFP1 (565/25, 630/60) were obtained from Chroma (Brattelboro, VT). One hour before imaging the culture medium was replaced with 20 mM HEPES-buffered minimal essential medium with Earle's salts without bicarbonate. During imaging the cells were maintained at 37 °C using a CSMI stage incubator (Harvard Apparatus). For each YFP-N-β·YFP-C-γ and GFP-β_1·CFP-γ combination, 40–70 cells were imaged from plates transfected on 3 different days.

Measurement of Intensity and Membrane Targeting of YFP-N-β·YFP-C-γ Complexes—The membrane marker (ECFP-Mem) was used as the primary criterion for selecting cells for imaging and analysis. Cells having a clear plasma membrane border and adjacent region of cytoplasm were identified. If the cell also had detectable intensity of the cytoplasm marker (mRFP) and YFP-N-β·YFP-C-γ, then the cell image was recorded. Exposure times and gain for each image varied depending on cell intensity, and the following corrections were made so that the intensity values correspond to a 1-s exposure, gain of 1, with instrument background subtracted. Instrument background as a function of exposure time and gain was determined from images of dishes containing media without cells. The instrument background was subtracted from each image, and the remaining intensity was scaled to correspond to an exposure time of 1 s and a gain of 1. Fluorescence intensity was determined empirically to be related linearly to exposure time and gain. A small amount of bleed-through of CFP intensity into the YFP images (0.6%) was then subtracted. All image processing was performed using IPlab software.

The average fluorescence intensity of each YFP-N-β·YFP-C-γ combination was determined by tracing the border of each cell using the ECFP-Mem image and calculating the average pixel intensity of the entire cell including the border for the YFP-N-β·YFP-C-γ image. The average intensity of YFP-C-γ_7, which does not contain the chromophore, expressed alone (7.5, S.E. = 0.16, n = 18) was used to determine the intensity due to autofluorescence. Images with average intensity values below 7.5 were not included in the calculation of average intensity or of plasma membrane fraction, described in the next paragraph.

The plasma membrane fraction of the YFP-N-β·YFP-C-γ complexes in each cell was determined as follows (see Fig. 6, *C–F*). Plasma membrane pixels corresponding to a length of plasma membrane were identified and marked using the ECFP-Mem image. Cytoplasm pixels were marked with a 12 × 12-pixel box adjacent to the plasma membrane pixels in a region that was devoid of intracellular membranes, which were not quantified. The plasma membrane to cytoplasm ratios of YFP-N-β·YFP-C-γ (βγR), plasma membrane marker (PMR), and cytoplasm marker (CR) were calculated by dividing the average intensity of each label in the marked plasma membrane region by the average intensity in the marked cytoplasm region. PMR and CR were very consistent, with mean values of 1.24 (S.D. = 0.15, n = 375) and 0.66 (S.D. = 0.099, n = 375), respectively. The plasma membrane fraction of YFP-N-β·YFP-C-γ, PMF(βγ), is defined as the plasma membrane to cytoplasm ratio of YFP-N-β·YFP-C-γ relative to that of the plasma membrane and cytoplasm markers in the same cell and was calculated using the following equation.

$$\mathrm{PMF}(\beta\gamma) = (\beta\gamma\mathrm{R} - \mathrm{CR})/(\mathrm{PMR} - \mathrm{CR})\,. \qquad \text{(Eq. 1)}$$

A value of zero corresponds to a completely cytoplasmic distribution, and a value of one corresponds to a completely plasma membrane distribution.

RESULTS

Development of a Method to Visualize Functional Fluorescent βγ Dimers—We have applied the strategy of BiFC (25) to visualize βγ dimers. This approach involves the production of a fluorescent signal by two nonfluorescent fragments of YFP when they are brought together by interactions between proteins fused to each fragment. The G protein β and γ subunits appeared to be ideal candidates for this technique because they associate irreversibly into a complex that functions as a single unit and the amino termini of the two subunits are associated into a coiled-coil (34). To produce fluorescent βγ dimers we fused an amino-terminal YFP fragment (residues 1–158, referred to as YFP-N) to the amino terminus of the β subunit to produce YFP-N-β and a carboxyl-terminal YFP fragment (residues 159–238, referred to as YFP-C) to the amino terminus of the γ subunit to produce YFP-C-γ (Fig. 1). As an initial test of this approach, one of us (L. T.) produced YFP-N-β and YFP-C-γ constructs derived from the single β and single γ subunits that are encoded in the genome of the cellular slime mold, *Dictyostelium discoideum*. Expressing both of these YFP-N-β and YFP-C-γ constructs resulted in a fluorescence signal that was enriched on the plasma membrane (Fig. 2 and Supplemental Video 1), whereas expressing either recombinant protein alone did not produce a detectable fluorescent signal (data not

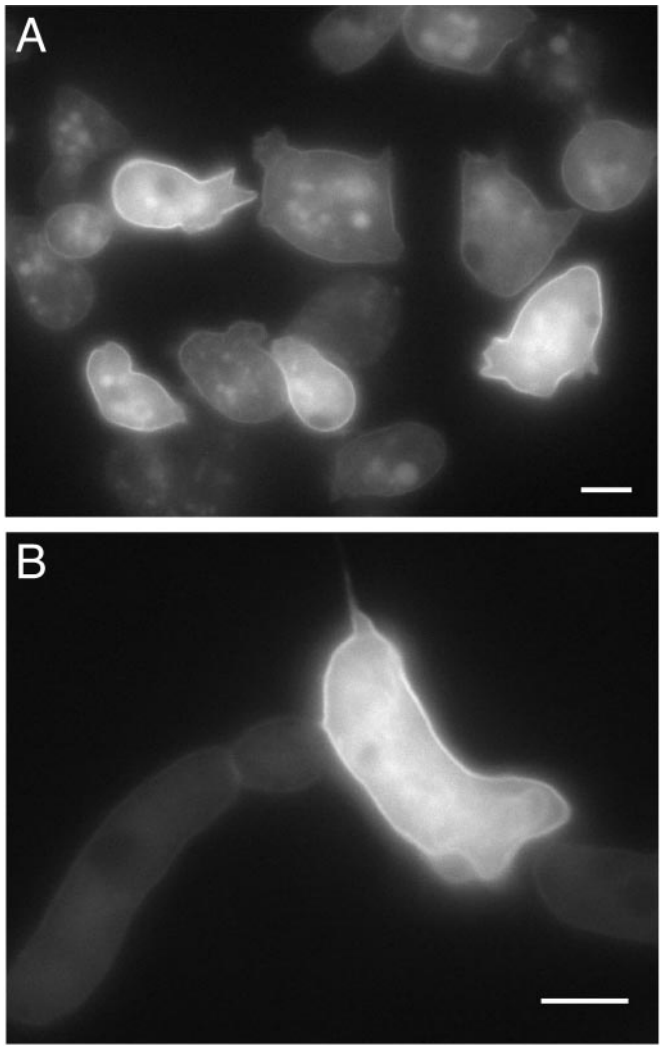

FIG. 2. **Imaging of YFP-N-β·YFP-C-γ in *D. discoideum*.** Wild-type *D. discoideum* Ax-3 cells were transformed by electroporation with YFP-N-β and YFP-C-γ, and transformants were selected using 20 μg/ml G418 in HL-5 media. *A*, distribution of YFP-N-β·YFP-C-γ in vegetative (growth phase) cells. *B*, distribution of YFP-N-β·YFP-C-γ in polarized chemotaxing cells. *D. discoideum* lives as a single cell organism when the environment is favorable, whereas adverse conditions such as starvation trigger aggregation of cells to form multicellular structures. During aggregation, chemotaxis of amoebae to cAMP secreted by other cells is mediated by a G protein-coupled receptor. In these chemotaxing cells YFP-N-β·YFP-C-γ complexes were also distributed uniformly around the plasma membrane. *Bar* = 5 μm. A video is available as supplemental material (Video 1). In this video, Ax-3 cells expressing YFP-N-β·YFP-C-γ were starved for 5 h before being exposed to a chemoattractant gradient produced with a micropipet filled with cAMP. The *circle* indicates the location of the micropipet tip.

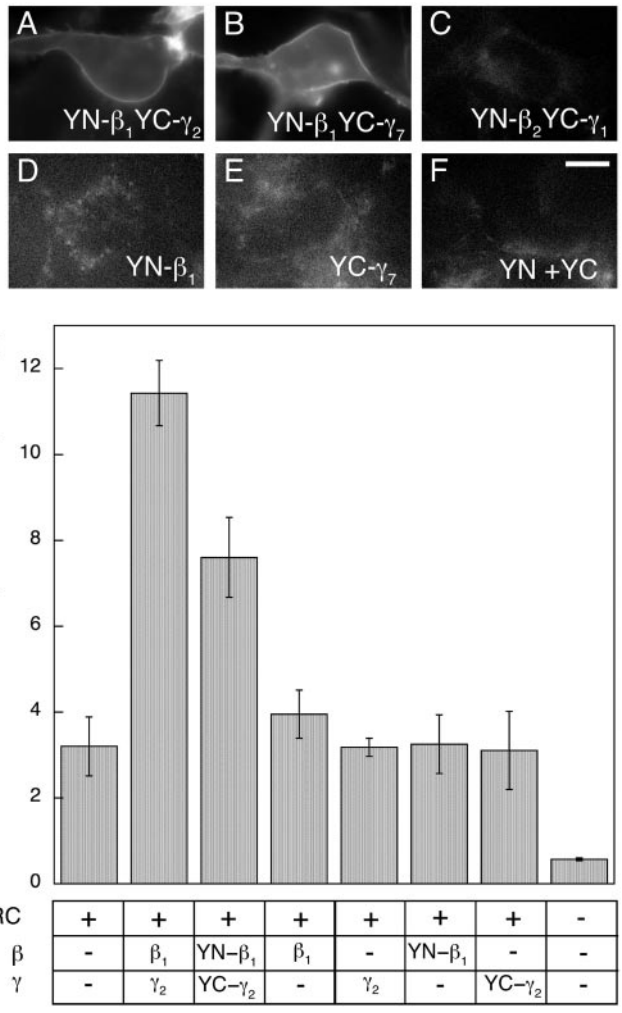

FIG. 3. **The BiFC approach produces specific fluorescence from functional βγ dimers.** YFP-N-β_1·YFP-C-γ_2 (*A*) and YFP-N-β_1·YFP-C-γ_7 (*B*) produce strong signals in the plasma membranes of HEK-293 cells. *C*, YFP-N-β_2·YFP-C-γ_1, which does not form a functional dimer (2, 35, 36), does not produce a specific fluorescent signal. When expressed by themselves, YFP-N-β_1 (*D*) and YFP-C-γ_7 (*E*) are not fluorescent. In addition, co-expression of YFP-N and YFP-C does not produce fluorescence (*F*). Considerable variation in signal strength required adjusting the brightness of the final images by plotting restricted ranges of the pixel values (normalized to a 1 s exposure) as follows: *A*, 5–80; *B*, 5–80; *C*, 4–12; *D*, 6–12; *E*, 6–12; *F*, 6–12. HEK-293 cells were transfected and imaged as described under "Experimental Procedures." *Bar* = 10 μm. *G*, YFP-N-β·YFP-C-γ dimers potentiate activation of adenylyl cyclase. The adenylyl cyclase activity in COS-7 cells is stimulated by βγ in the presence of activated α_s (37). cAMP accumulation was measured in COS-7 cells transfected with a total of 2.025 μg of plasmid consisting of vector alone (pcDNAI/Amp) or varying amounts of vector plus 0.025 μg of plasmid encoding α_sR201C (56), a constitutively activated α_s mutant (38), and 1 μg each of plasmids encoding the indicated β and γ subunits. *YN* indicates YFP-N, and *YC* indicates YFP-C. Values represent the means ± S.E. of 3–6 independent experiments performed in triplicate.

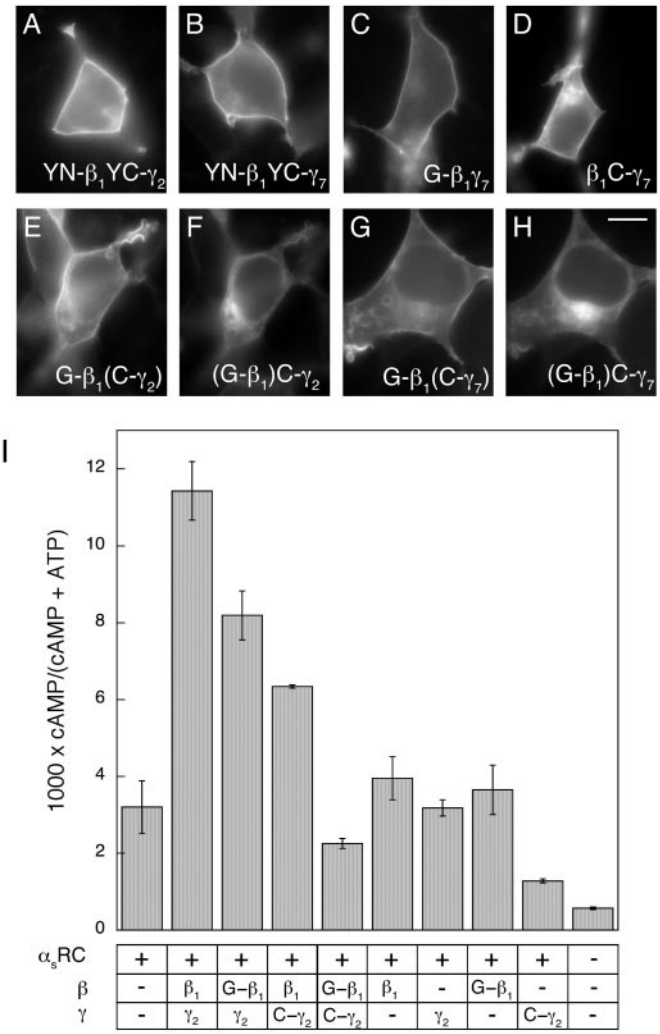

FIG. 4. **Comparison of YFP-N-β·YFP-C-γ dimers with those produced using GFP-β and CFP-γ.** *A–H*, YFP-N-β·YFP-C-γ dimers produce more specific labeling of the plasma membrane than GFP-β·CFP-γ dimers. HEK-293 cells expressing the following constructs were imaged. *A*, YFP-N-β_1·YFP-C-γ_2. *B*, YFP-N-β_1·YFP-C-γ_7. *C*, GFP-β_1·γ_7. *D*, β_1·CFP-γ_7. *E* and *F*, same cell: *E*, GFP-β_1 (co-expressed with CFP-γ_2); *F*, CFP-γ_2 (co-expressed with GFP-β_1). *G* and *H*, same cell: *G*, GFP-β_1 (co-expressed with CFP-γ_7); *H*, CFP-γ_7 (co-expressed with GFP-β_1). *Bar* = 10 μm. *I*, GFP-β·γ and β·CFP-γ, but not GFP-β·CFP-γ, dimers potentiate activation of adenylyl cyclase in COS-7 cells. cAMP accumulation was measured in COS-7 cells transfected with a total of 2.025 μg of plasmid consisting of vector alone (pcDNAI/Amp) or varying amounts of vector plus 0.025 μg of plasmid encoding α_sR201C and 1 μg each of plasmids encoding the indicated β and γ subunits. *YN* indicates YFP-N, *YC* indicates YFP-C, *G* indicates GFP, and *C* indicates CFP. Values represent the means ± S.E. of 3–6 independent experiments performed in triplicate.

shown). This result demonstrates that BiFC can be used to image βγ dimers and led us to investigate whether this approach could distinguish among the numerous potential βγ dimers formed in mammals in terms of their efficiency of formation and their subcellular localization patterns.

To test the ability of the BiFC approach to produce functional fluorescent βγ dimers, we examined the properties of YFP-N-β_1·YFP-C-γ_2 and YFP-N-β_1·YFP-C-γ_7 complexes. $\beta_1\gamma_2$ has been used extensively in studies of interactions between βγ and effectors such as adenylyl cyclase (2), phospholipase C (3), and G protein-gated inwardly rectifying K^+ channels (4). Ribozyme inactivation studies have shown that $\beta_1\gamma_7$ mediates signaling from the β_2-adrenergic receptor to adenylyl cyclase via G_s in HEK-293 cells (11, 12). YFP-N-β_1·YFP-C-γ_2 (Fig. 3*A*) and YFP-N-β_1·YFP-C-γ_7 (Fig. 3*B*) exhibited strong signals in the plasma membrane. However, when expressed by themselves, YFP-N-β_1 (Fig. 3*D*) and YFP-C-γ_7 (Fig. 3*E*) were not fluorescent. In addition, co-expression of YFP-N and YFP-C did not produce a specific fluorescent signal (Fig. 3*F*). Specific fluorescence was not obtained upon co-expression of YFP-N-β_2 and YFP-C-γ_1 (Figs. 3*C*, 5*D*, and 6*A*), confirming previous studies indicating that β_2 and γ_1 do not interact to form a functional dimer (2, 35, 36). These results indicate that the BiFC method only produces specific fluorescence when YFP-N and YFP-C are fused to β and γ subunits that interact.

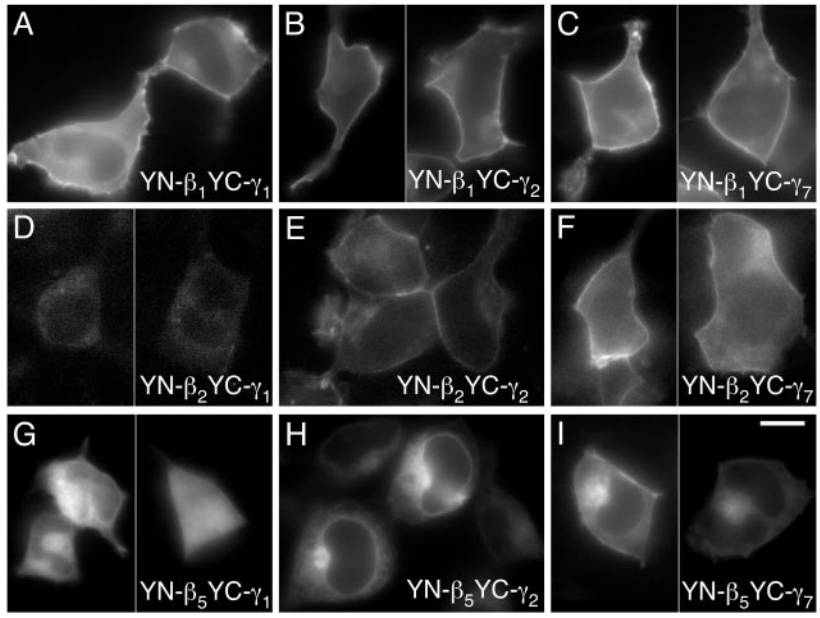

FIG. 5. **BiFC applied to imaging different βγ complexes.** Images *A–I* represent different YFP-N-β·YFP-C-γ combinations expressed in HEK-293 cells. *A*, YFP-N-β_1·YFP-C-γ_1; *B*, YFP-N-β_1·YFP-C-γ_2; *C*, YFP-N-β_1·YFP-C-γ_7; *D*, YFP-N-β_2·YFP-C-γ_1; *E*, YFP-N-β_2·YFP-C-γ_2; *F*, YFP-N-β_2·YFP-C-γ_7; *G*, YFP-N-β_5·YFP-C-γ_1; *H*, YFP-N-β_5·YFP-C-γ_2; *I*, YFP-N-β_5·YFP-C-γ_7. *Bar* = 10 μm. *YN* indicates YFP-N, and *YC* indicates YFP-C. Considerable variation in signal strength (quantified in Fig. 6*A*) required adjusting the brightness of the final images by plotting restricted ranges of the pixel values (normalized to a 1-s exposure) as follows. *A*, 5–140; *B*, 5–120; *C*, 5–140; *D*, 5–15; *E*, 5–24; *F*, 5–24; *G*, 5–80; *H*, 5–120; *I*, 5–70.

Functionality of BiFC βγ complexes was tested for by determining their abilities to modulate adenylyl cyclase activity. The adenylyl cyclase activity in COS-7 cells is stimulated by βγ in the presence of activated α_s (37). cAMP accumulation was measured in COS-7 cells that co-expressed α_sR201C, a constitutively activated α_s mutant (38), and fluorescent or unlabeled βγ complexes. YFP-N-β_1·YFP-C-γ_2 potentiated adenylyl cyclase activation with a somewhat lower efficacy than did $\beta_1\gamma_2$, whereas individually expressed β and γ subunits did not potentiate activation of adenylyl cyclase (Fig. 3*G*). Comparisons of expression levels in immunoblots of membranes of COS-7 cells transfected with either $\beta_1\gamma_2$ or YFP-N-β_1·YFP-C-γ_2 showed that attachment of YFP-C to γ_2 had only minor effects on expression, but attachment of YFP-N to β_1 resulted in a decreased level of expression (data not shown), which could account for the decreased activity of YFP-N-β_1·YFP-C-γ_2 compared with that of $\beta_1\gamma_2$. Similar results were obtained with YFP-N-β_1·YFP-C-γ_7 (data not shown).

Comparison of BiFC βγ Dimers with Those Obtained Using GFP-β and CFP-γ—Imaging of YFP-N-β·YFP-C-γ complexes ensures that only β and γ subunits that are associated as a dimer are visualized, whereas imaging of co-expressed GFP-β and CFP-γ subunits results in visualization of the total amount of β and γ subunits expressed in a cell. The plasma membrane signal exhibited by cells expressing YFP-N-β·YFP-C-γ complexes (Fig. 4, *A* and *B*) represented a greater percentage of the total signal than that in cells that co-expressed GFP-β_1 and either CFP-γ_2 (Fig. 4, *E* and *F*) or CFP-γ_7 (Fig. 4, *G* and *H*). Moreover, the cytosolic GFP-β_1 and CFP-γ signals did not co-localize entirely. The β signal tended to be more diffuse, whereas the γ signal generally was attached to intracellular vesicles and membranes. This is consistent with the fact that the γ subunit, but not the β subunit, is prenylated, resulting in membrane attachment. When GFP-β_1 was co-expressed with unlabeled γ_7 (Fig. 4*C*) and when CFP-γ_7 was co-expressed with unlabeled β_1 (Fig. 4*D*), the relative amounts of signal in the plasma membrane were greater than when the two labeled constructs were co-expressed (Fig. 4, *G* and *H*). These results suggest that GFP-β and CFP-γ subunits do not assemble together into dimers.

Also in contrast to the BiFC approach, fusion of GFP derivatives to both β and γ did not result in βγ dimers that could potentiate activation of adenylyl cyclase. The activities of GFP-β_1·γ_2 and β_1·CFP-γ_2 (Fig. 4I) were similar to that of YFP-N-β_1·YFP-C-γ_2 (Fig. 3*G*), but GFP-β_1·CFP-γ_2 was not functional (Fig. 4I). However, as determined in immunoblots of membranes of COS-7 cells transfected with either YFP-N-β_1·YFP-C-γ_2 or GFP-β_1·CFP-γ_2, GFP-β_1 was expressed at the same level as was YFP-N-β_1, and CFP-γ_2 was expressed at a higher level than was YFP-C-γ_2 (data not shown). Corresponding results were obtained with GFP-β_1·γ_7, β_1·CFP-γ_7, and GFP-β_1·CFP-γ_7 complexes (data not shown). Most likely, this indicates that, whereas the βγ complex can tolerate fusion of a single GFP molecule to the amino terminus of β or γ, attachment of GFP to the amino termini of both subunits disrupts proper folding.

Imaging of BiFC βγ Dimers Indicates Roles for Both β and γ in Targeting—To investigate whether different β and γ combinations can be distinguished *in vivo* in terms of their abilities to form dimers, we imaged HEK-293 cells expressing pairwise combinations of YFP-N-β_1, YFP-N-β_2, and YFP-N-β_5, with YFP-C-γ_1, YFP-C-γ_2, and YFP-C-γ_7 (Fig. 5). There were clear differences in the average intensities of different βγ dimers (Fig. 6*A*). Based on these average intensities, complexes containing β_1 and β_5, with the exception of $\beta_5\gamma_1$, were formed to a greater extent than complexes containing β_2. As described above, application of BiFC to β_2 and γ_1, which do not interact to form a functional dimer (2, 35, 36), did not produce specific fluorescence (Figs. 5*D* and 6*A*). However, both YFP-N-β_2 (Fig. 5, *E* and *F*) and YFP-C-γ_1 (Fig. 5, *A* and *G*) produced fluorescent complexes upon co-expression with other binding partners.

Different YFP-N-β·YFP-C-γ complexes exhibited distinguishable localization patterns (Figs. 5 and 6*B*). A distinct plasma membrane signal was obtained with YFP-N-β_1·YFP-C-γ_1, the βγ complex associated with transducin (Fig. 5*A*), and with YFP-N-β_1·YFP-C-γ_2 (Fig. 5*B*), YFP-N-β_1·YFP-C-γ_7 (Fig. 5*C*), YFP-N-β_2·YFP-C-γ_2 (Fig. 5*E*), and YFP-N-β_2·YFP-C-γ_7 (Fig. 5*F*), which have similar abilities to modulate the activities of adenylyl cyclase and phospholipase C (3). As quantified in Fig. 6, YFP-N-β_1·YFP-C-γ_7 exhibited the greatest amount of signal in the plasma membrane compared with the cytoplasm followed by YFP-N-β_1·YFP-C-γ_2 and then YFP-N-β_1·YFP-C-γ_1 and YFP-N-β_2·YFP-C-γ_2. In contrast, none of the β_5 complexes localized primarily to the plasma membrane. YFP-N-β_5·YFP-C-γ_1 (Fig. 5*G*) predominantly exhibited a diffuse cytosolic pattern. YFP-N-β_5·YFP-C-γ_2 (Fig. 5*H*) targeted to intracellular

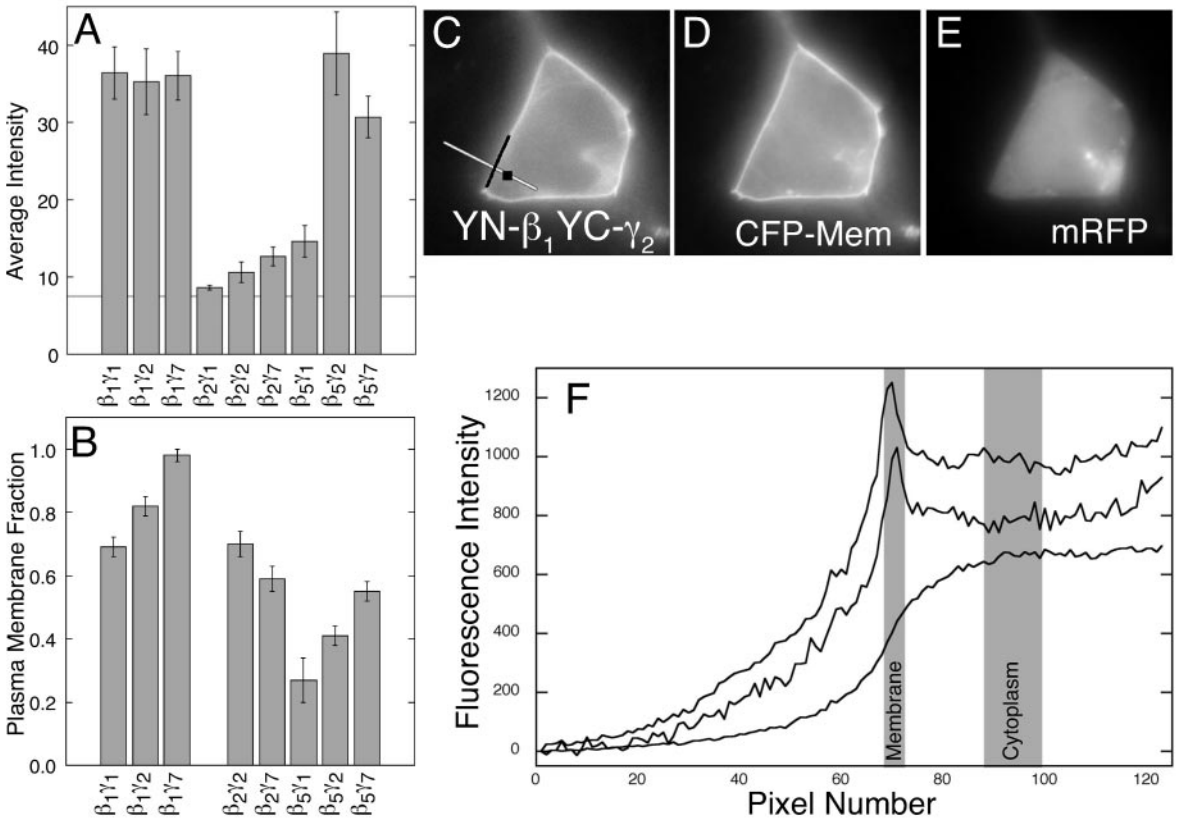

FIG. 6. **Quantitative comparisons of YFP-N-β·YFP-C-γ images.** *A*, average fluorescence intensities of the different YFP-N-β·YFP-C-γ complexes. Intensity values correspond to a 1-s exposure with instrument background subtracted. The line at *Average Intensity* = 7.5 represents the value of YFP-C-γ_7 expressed alone. Because this YFP fragment does not contain the chromophore, this represents cellular autofluorescence, and images with values below this were not included in this analysis. $\beta_2\gamma_1$, which does not form a functional dimer (2, 35, 36), exhibited a value just above this cut-off (8.62, S.E. = 0.31) in 8/46 images, whereas the other images collected for this combination fell below this cut-off. For comparison, 63/68 of $\beta_1\gamma_1$ images, 52/54 of $\beta_1\gamma_2$ images, 59/62 of $\beta_1\gamma_7$ images, 31/54 $\beta_2\gamma_2$ images, 28/56 $\beta_2\gamma_7$ images, 20/56 $\beta_5\gamma_1$ images, 51/52 $\beta_5\gamma_2$ images, and 63/74 $\beta_5\gamma_7$ images had intensities above this cut-off. Values represent the mean intensities ± S.E. of the images above the autofluorescence cut-off. *B*, plasma membrane fractions of the YFP-N-β·YFP-C-γ complexes. As described under "Experimental Procedures," cytoplasm intensity was measured in a region adjacent to the plasma membrane that was devoid of intracellular membranes, which were not quantified. A value of zero corresponds to a completely cytoplasmic distribution, and a value of one corresponds to a completely plasma membrane distribution. The plasma membrane fraction of $\beta_2\gamma_1$ is not included because the intensity of this combination was generally below the autofluorescence cut-off. Values represent the mean ± S.E. of determinations using the same images with intensities above the autofluorescence cut-off as were used in *A*. *C–F*, illustration of plasma membrane fraction measurement using the cell shown in Fig. 4*A*. *C*, image of YFP-N-β_1·YFP-C-γ_2 with a *black line* marking the membrane pixels and a *black square* marking the cytoplasm pixels. A *white line* indicates the location of pixel intensities shown in *F*. *YN* indicates YFP-N, and *YC* indicates YFP-C. *D*, image of ECFP-Mem (plasma membrane marker). *E*, image of mRFP (cytoplasm marker); *F*, plot of fluorescence intensity along *white line* indicated in *C*. *Top curve*, ECFP-Mem; *middle curve*, YFP-N-β_1·YFP-C-γ_2; *bottom curve*, mRFP. The location of the membrane pixels and cytoplasm pixels are indicated by the *gray bars*. The fluorescence intensities were scaled for clarity.

membranes, which appeared to include Golgi membranes, the endoplasmic reticulum, and the nuclear membrane, whereas YFP-N-β_5·YFP-C-γ_7 (Fig. 5I) exhibited some signal in intracellular membranes, although generally not the nuclear membrane, and also some signal in the plasma membrane. As discussed below, the different localization patterns obtained with specific βγ complexes indicate that both β and γ play roles in determining subcellular localization.

DISCUSSION

We have applied the strategy of BiFC (25) to image complexes of β and γ subunits. This strategy takes advantage of the ability of two nonfluorescent fragments of YFP to form a fluorescent signal when fused to the amino termini of β and γ subunits, which form a coiled-coil in the βγ structure (34). This method of imaging βγ subunits is superior to imaging β and γ subunits that are individually tagged with GFP derivatives for several reasons. First, individually tagged β and γ, when expressed together, are unable to modulate the activity of adenylyl cyclase, although each is functional when co-expressed with an untagged binding partner, indicating that simultaneously placing GFP derivatives at the amino termini of both β and γ is disruptive. This result suggests that FRET experiments using CFP and YFP-tagged β and γ subunits are not optimal ways to measure assembly of functional dimers, although in assays of calcium channel regulation functionality of such dimers has been reported (39, 40). Second, the localization patterns of βγ complexes imaged using BiFC differ from those of individually tagged subunits, generally exhibiting a more pronounced plasma membrane localization. In addition to localizing to the plasma membrane, GFP-β_1 displayed a diffuse cytosolic pattern, whereas CFP-γ_2 and CFP-γ_7 localized to intracellular membranes. Because β and γ are only functional when assembled into dimers, these additional locations of individually tagged subunits may either reflect unassembled proteins targeted for degradation or complexes of labeled proteins with endogenous binding partners. In contrast, the BiFC method ensures that only specific functional βγ complexes are visualized. We have demonstrated that this method can be used to determine which β and γ subunits form complexes *in vivo* and to compare the relative amounts of complex formation and

subcellular localization patterns of different complexes.

Taken together with previous studies our results indicate that the G protein α, β, and γ subunits all play roles in mutually targeting each other to the plasma membrane. Our studies indicate a role for the β subunit in targeting γ in that complexes containing β_1 and β_2 localized to the plasma membrane, whereas those containing β_5 accumulated in the cytosol or on intracellular membranes. Previously, βγ was demonstrated to play a role in targeting the α subunit in that specific βγ combinations exhibited differing abilities to restore plasma membrane targeting to α_s and α_q mutants with decreased abilities to interact with βγ (20), and a γ subunit targeted to the mitochondria caused α and β to mislocalize (23). Conversely, under certain conditions co-expression of α_s is required to target $\beta_1\gamma_2$ to the plasma membrane, and an α_s mutant that is targeted to the mitochondria brings $\beta_1\gamma_2$ with it (24).

The different localization patterns obtained with specific βγ complexes indicate that both β and γ play roles in determining subcellular localization. Based on the complexes we have studied, these roles appear to be distinct. Comparisons of dimers containing different β subunits indicate a role for the β subunit in determining whether the dimer localizes to the plasma membrane or intracellular membranes. In contrast, the γ subunit generally determined the degree of membrane association but did not specify whether the dimer localized to the plasma membrane or intracellular membranes. Dimers containing γ_2 or γ_7 associated with membranes to a greater extent than those containing γ_1, consistent with the fact that γ_1 is farnesylated, whereas the other γ subunits are gernanylgeranylated. The 20-carbon isoprenoid geranylgeranyl is more hydrophobic than the 15-carbon farnesyl group and $\beta_1\gamma_1$, but not geranylgeranylated βγ dimers, are soluble in the absence of detergents (22). However, in the context of β_5, the γ subunit also played a role in determining to which membranes the dimer localized in that $\beta_5\gamma_2$ and $\beta_5\gamma_7$ exhibited distinguishable membrane localization patterns. Perhaps in the case of $\beta_5\gamma$ compared with $\beta_1\gamma$ and $\beta_2\gamma$ dimers, the γ subunit plays a more dominant role in membrane targeting because β_5 exhibits relatively weak interactions with endogenous α subunits, as discussed below.

Localization of $\beta_5\gamma$ dimers to intracellular membranes rather than the plasma membrane could either indicate a direct targeting role for β or an indirect role related to association with α subunits. Previous studies suggest that palmitoylation of the α subunit is important for plasma membrane targeting because efficient plasma membrane targeting of $\beta_1\gamma_2$ expressed in HEK-293 cells required either co-expression of α_s or introduction of a palmitoylation site into γ_2 (24). We observed efficient localization of BiFC $\beta_1\gamma_2$ to the plasma membrane in the absence of co-expressed α subunits, but this could be due to association with endogenous α subunits. Based on fluorescence intensity, the $\beta_5\gamma$ dimers were expressed at similar or lower levels compared with other βγ dimers that associated primarily with the plasma membrane. However, since $\beta_5\gamma_2$ interacts with α_q, but not other α subunits *in vitro* (41), relatively weak interactions with endogenous α subunits might explain the localization pattern observed for $\beta_5\gamma$ dimers. One model for targeting of αβγ heterotrimers, based on a study in which CFP-α_{i2} and YFP-γ_2 co-localized in both the region of the Golgi apparatus and the plasma membrane (42), proposes that α and βγ associate on the Golgi apparatus, where the α subunit is palmitoylated, leading to targeting of the heterotrimer to the plasma membrane. Future studies will investigate the potential role of α subunits in regulating localization of $\beta_5\gamma$ dimers.

Functionality of $\beta_5\gamma_2$ dimers has been demonstrated in that they can inhibit G protein-gated inwardly rectifying K^+ channels (43) and activate phospholipase C. Both $\beta_5\gamma_1$ (44) and $\beta_5\gamma_7$ (45) can also stimulate phospholipase C, but only modestly compared with $\beta_5\gamma_2$. However, when purified from native tissues, β_5 is associated with RGS proteins that contain Gγ-like domains, such as RGS7, with which it is associated in the brain (46). In PC12 cells, endogenously expressed β_5 and RGS7 co-localize in the nucleus (47). Interaction with RGS7 is required for nuclear localization because β_5 mutants that can dimerize with γ_2, but not RGS7, are excluded from the nucleus (48). In addition, co-expression of β_5 and RGS6 promotes co-localization of both proteins in the nucleus (49). Our demonstration that $\beta_5\gamma$ complexes localize to intracellular membranes, including the nuclear membrane, but are excluded from the nucleus itself is consistent with these previous studies. Future studies will directly compare the localization of β_5 when complexed with either γ subunits or RGS proteins with Gγ-like domains.

In some cases, differential localization patterns of G protein subunits may be due to differences in their association with membrane microdomains such as caveolae and focal adhesions (50–52). Cell-specific expression of these membrane domains may be responsible for differences in G protein subunit association observed in different cell types (53). In turn, differences in heterotrimer composition may account for cell-specific effects of receptors as well as the diverse cellular effects of receptors that apparently couple to the same G proteins. Application of the BiFC method to visualize specific βγ dimers in a wide variety of cells and tissues with distinctive morphologies will help to elucidate the ways in which subcellular localization can regulate signaling pathways.

Acknowledgments—We thank Janet Robishaw for plasmids expressing β and γ subunits, Thomas Hughes for the pWay5 vector, and Roger Tsien for the mRFP plasmid. We also thank Jennifer Malcolm for producing the YFP-(1–158)β_2 expression plasmid. In addition, we thank Drs. Robishaw and Hughes for helpful discussions and critical reading of the manuscript.

REFERENCES

1. Hurowitz, E. H., Melnyk, J. M., Chen, Y. J., Kouros-Mehr, H., Simon, M. I., and Shizuya, H. (2000) *DNA Res.* **7,** 111–120
2. Iniguez-Lluhi, J. A., Simon, M. I., Robishaw, J. D., and Gilman, A. G. (1992) *J. Biol. Chem.* **267,** 23409–23417
3. Ueda, N., Iniguez-Lluhi, J. A., Lee, E., Smrcka, A. V., Robishaw, J. D., and Gilman, A. G. (1994) *J. Biol. Chem.* **269,** 4388–4395
4. Mirshahi, T., Robillard, L., Zhang, H., Hebert, T. E., and Logothetis, D. E. (2002) *J. Biol. Chem.* **277,** 7348–7355
5. Robishaw, J. D., and Berlot, C. H. (2004) *Curr. Opin. Cell Biol.* **16,** 206–209
6. Kleuss, C., Hescheler, J., Ewel, C., Rosenthal, W., Schultz, G., and Wittig, B. (1991) *Nature* **353,** 43–48
7. Kleuss, C., Scherubl, H., Hescheler, J., Schultz, G., and Wittig, B. (1992) *Nature* **358,** 424–426
8. Kleuss, C., Scherubl, H., Hescheler, J., Schultz, G., and Wittig, B. (1993) *Science* **259,** 832–834
9. Macrez-Lepretre, N., Kalkbrenner, F., Morel, J. L., Schultz, G., and Mironneau, J. (1997) *J. Biol. Chem.* **272,** 10095–10102
10. Dippel, E., Kalkbrenner, F., Wittig, B., and Schultz, G. (1996) *Proc. Natl. Acad. Sci. U. S. A.* **93,** 1391–1396
11. Wang, Q., Mullah, B. K., and Robishaw, J. D. (1999) *J. Biol. Chem.* **274,** 17365–17371
12. Wang, Q., Mullah, B., Hansen, C., Asundi, J., and Robishaw, J. D. (1997) *J. Biol. Chem.* **272,** 26040–26048
13. Schwindinger, W. F., Betz, K. S., Giger, K. E., Sabol, A., Bronson, S. K., and Robishaw, J. D. (2003) *J. Biol. Chem.* **278,** 6575–6579
14. Richardson, M., and Robishaw, J. D. (1999) *J. Biol. Chem.* **274,** 13525–13533
15. Figler, R. A., Lindorfer, M. A., Graber, S. G., Garrison, J. C., and Linden, J. (1997) *Biochemistry* **36,** 16288–16299
16. Butkerait, P., Zheng, Y., Hallak, H., Graham, T. E., Miller, H. A., Burris, K. D., Molinoff, P. B., and Manning, D. R. (1995) *J. Biol. Chem.* **270,** 18691–18699
17. Hou, Y., Azpiazu, I., Smrcka, A., and Gautam, N. (2000) *J. Biol. Chem.* **275,** 38961–38964
18. Hou, Y., Chang, V., Capper, A. B., Taussig, R., and Gautam, N. (2001) *J. Biol. Chem.* **276,** 19982–19988
19. Robishaw, J. D., Schwindinger, W. F., and Hansen, C. A. (2003) *Handbook of Cell Signaling*, Vol. 2, pp. 623–629, Academic Press, Elsevier
20. Evanko, D. S., Thiyagarajan, M. M., Siderovski, D. P., and Wedegaertner, P. B. (2001) *J. Biol. Chem.* **276,** 23945–23953
21. Simonds, W. F., Butrynski, J. E., Gautam, N., Unson, C. G., and Spiegel, A. M. (1991) *J. Biol. Chem.* **266,** 5363–5366

22. Wedegaertner, P. B., Wilson, P. T., and Bourne, H. R. (1995) *J. Biol. Chem.* **270,** 503–506
23. Fishburn, C. S., Pollitt, S. K., and Bourne, H. R. (2000) *Proc. Natl. Acad. Sci. U. S. A.* **97,** 1085–1090
24. Takida, S., and Wedegaertner, P. B. (2003) *J. Biol. Chem.* **278,** 17284–17290
25. Hu, C. D., Chinenov, Y., and Kerppola, T. K. (2002) *Mol. Cell* **9,** 789–798
26. Griesbeck, O., Baird, G. S., Campbell, R. E., Zacharias, D. A., and Tsien, R. Y. (2001) *J. Biol. Chem.* **276,** 29188–29194
27. Ray, K., Kunsch, C., Bonner, L. M., and Robishaw, J. D. (1995) *J. Biol. Chem.* **270,** 21765–21771
28. Lo, W., Rodgers, W., and Hughes, T. (1998) *Biotechniques* **25,** 94–96 and 98
29. Miyawaki, A., Griesbeck, O., Heim, R., and Tsien, R. Y. (1999) *Proc. Natl. Acad. Sci. U. S. A.* **96,** 2135–2140
30. Manahan, C. L., Patnana, M., Blumer, K. J., and Linder, M. E. (2000) *Mol. Biol. Cell* **11,** 957–968
31. Medina, R., Grishina, G., Meloni, E. G., Muth, T. R., and Berlot, C. H. (1996) *J. Biol. Chem.* **271,** 24720–24727
32. Skene, J. H., and Virag, I. (1989) *J. Cell Biol.* **108,** 613–624
33. Campbell, R. E., Tour, O., Palmer, A. E., Steinbach, P. A., Baird, G. S., Zacharias, D. A., and Tsien, R. Y. (2002) *Proc. Natl. Acad. Sci. U. S. A.* **99,** 7877–7882
34. Sondek, J., Bohm, A., Lambright, D. G., Hamm, H. E., and Sigler, P. B. (1996) *Nature* **379,** 369–374
35. Pronin, A. N., and Gautam, N. (1992) *Proc. Natl. Acad. Sci. U. S. A.* **89,** 6220–6224
36. Schmidt, C. J., Thomas, T. C., Levine, M. A., and Neer, E. J. (1992) *J. Biol. Chem.* **267,** 13807–13810
37. Federman, A. D., Conklin, B. R., Schrader, K. A., Reed, R. R., and Bourne, H. R. (1992) *Nature* **356,** 159–161
38. Landis, C. A., Masters, S. B., Spada, A., Pace, A. M., Bourne, H. R., and Vallar, L. (1989) *Nature* **340,** 692–696
39. Ruiz-Velasco, V., and Ikeda, S. R. (2001) *J. Physiol.* (*Lond.*) **537,** 679–692
40. Zhou, J. Y., Toth, P. T., and Miller, R. J. (2003) *J. Pharmacol. Exp. Ther.* **305,** 460–466
41. Fletcher, J. E., Lindorfer, M. A., DeFilippo, J. M., Yasuda, H., Guilmard, M., and Garrison, J. C. (1998) *J. Biol. Chem.* **273,** 636–644
42. Michaelson, D., Ahearn, I., Bergo, M., Young, S., and Philips, M. (2002) *Mol. Biol. Cell* **13,** 3294–3302
43. Lei, Q., Jones, M. B., Talley, E. M., Schrier, A. D., McIntire, W. E., Garrison, J. C., and Bayliss, D. A. (2000) *Proc. Natl. Acad. Sci. U. S. A.* **97,** 9771–9776
44. Watson, A. J., Katz, A., and Simon, M. I. (1994) *J. Biol. Chem.* **269,** 22150–22156
45. Zhang, S., Coso, O. A., Lee, C., Gutkind, J. S., and Simonds, W. F. (1996) *J. Biol. Chem.* **271,** 33575–33579
46. Witherow, D. S., Wang, Q., Levay, K., Cabrera, J. L., Chen, J., Willars, G. B., and Slepak, V. Z. (2000) *J. Biol. Chem.* **275,** 24872–24880
47. Zhang, J. H., Barr, V. A., Mo, Y., Rojkova, A. M., Liu, S., and Simonds, W. F. (2001) *J. Biol. Chem.* **276,** 10284–10289
48. Rojkova, A. M., Woodard, G. E., Huang, T. C., Combs, C. A., Zhang, J. H., and Simonds, W. F. (2003) *J. Biol. Chem.* **278,** 12507–12512
49. Chatterjee, T. K., Liu, Z., and Fisher, R. A. (2003) *J. Biol. Chem.* **278,** 30261–30271
50. Ostrom, R. S. (2002) *Mol. Pharmacol.* **61,** 473–476
51. Hansen, C. A., Schroering, A. G., Carey, D. J., and Robishaw, J. D. (1994) *J. Cell Biol.* **126,** 811–819
52. Ueda, H., Saga, S., Shinohara, H., Morishita, R., Kato, K., and Asano, T. (1997) *J. Cell Sci.* **110,** 1503–1511
53. Asano, T., Morishita, R., Ueda, H., and Kato, K. (1999) *J. Biol. Chem.* **274,** 21425–21429
54. Ormo, M., Cubbitt, A. B., Kallio, K., Gross, L. A., Tsien, R. Y., and Remington, S. J. (1996) *Science* **273,** 1392–1395
55. Lambright, D. G., Sondek, J., Bohm, A., Skiba, N. P., Hamm, H. E., and Sigler, P. B. (1996) *Nature* **379,** 311–319
56. Grishina, G., and Berlot, C. H. (1997) *J. Biol. Chem.* **272,** 20619–20626